Journal of the Physical Society of Japan
Vol. 71, No. 10, October, 2002, pp. 2357–2360

Simple Dynamical Model with History Dependence

Shuji ISHIHARA* and Kunihiko KANEKO

Department of Pure and Applied Sciences University of Tokyo, Komaba, Meguro-ku, Tokyo 153

(Received May 27, 2002)

A lattice dynamics model exhibiting history dependence is proposed, inspired by recent sandpile experiments. The stress distribution depends on the preparation process, which is explained as the dependence of certain attractors on the preparation conditions of the system. The model has three phases, but the history dependence is shown to exist only in the phase where a perturbation is amplified selectively rather than globally when propagating in the downflow direction. The condition for this history dependence is given in terms of the spatial Lyapunov exponent.

KEYWORDS: history dependence, nonlinearity, lattice dynamical system
DOI: 10.1143/JPSJ.71.2357

Physical systems exhibiting ''history dependence'' in the sense that their state is not solely determined by existing environmental conditions but is dependent on how the system was externally driven in the past are not uncommon. Examples of such systems can be found among glasses, polymers, and granular materials,[1] as well as in biological systems. Although hysteresis between two states is the simplest form of history dependence, here we examine cases where the evolution of a system may lead to many different states. In a dynamical system, each memory state can be interpreted as a different attractor. Hence, it is necessary to study how each attractor is selected and how feasible it is for one attractor to switch to another attractor. In order to do so, we consider a spatially extended system, and discuss the macroscopic features of history dependence.

An example of history dependence is given by recent sandpile experiments.[2,3] In these experiments, it was found that the pressure profile formed by stress chains in a sand pile strongly depends on how the sand grains are piled. Some particle simulations at the microscopic level reproduce the stress distribution,[9] while a theoretical study of stationary stress distribution has been proposed.[4–8] So far, neither the dynamical aspect nor the condition for such history dependence is clarified. In the present letter, we present a simple lattice dynamics model for studying the relationship of slow relaxation with history dependence. The model is inspired by the sandpile experiments, but we do not intend to propose an actual model for the experimental works. Rather, we try to extract a general condition for history dependence on dynamical systems.

In our toy model, we consider a mesoscopic approach by using a coarse-grained stress field instead of taking a variable for each grain position. A 'stress variable' x_{ij} is assigned to each site located on a two-dimensional triangular lattice (i,j). Due to gravity, the stress increases from the upper to the lower layer, while each site is associated with an intrinsic gravitational weight. The stress at a site (i,j) is transferred downwards by distributing the stress and the weight β_{ij} to the right and left neighbor sites in the next layer. The amount of stress transferred to the two lower sites is assumed to depend on the stress values of the sites as a given function, so that the ratio is given by $f(x_{rj+1}) : f(x_{lj+1})$.[10] ($r$ and l represent right and left, respectively, i.e., $l = j$ for even j and $l = j-1$ for odd j with $r = l+1$)

Based on these arguments, we introduce the following model of coupled differential equations:

$$\tau \frac{dx_{ij}(t)}{dt} = -x_{ij}(t) + \beta_{ij} + x_{l_ij-1}(t)\frac{f(x_{ij}(t))}{f(x_{ij}(t)) + f(x_{i-1j}(t))} + x_{r_i+x_{r_{ij}-1}}(t)\frac{f(x_{ij}(t))}{f(x_{ij}(t)) + f(x_{i+1j}(t))}, \quad (1)$$

where site $(l,j-1)$ is in the upper left and site $(r,j-1)$ is in the upper right of site (i,j). The time scale τ can be set to 1, by rescaling the time. We consider a homogeneous case here with a constant $\beta_{ij} = \beta$ (which can be set to 1 by rescaling the variable x). The lattice size, unless mentioned otherwise, is chosen to be N in the horizontal direction under periodic boundary conditions, and M in the vertical direction (sites in both the horizontal and vertical directions are numbered from 0 and hence $j = M-1$ denotes the bottom layer[10]).

The function $f(x)$ indicates the 'strength of competition' of the state under stress. We assume that the larger the stress of a site is, the more rigid its state is, and the more mass from the upper site it can support.[11] As an example, we adopt $f(x) = x^\alpha$ where α is a positive parameter that characterizes this reinforcement. Note, however, that this specific choice of $f(x)$ is not important, and the results to be presented are universal as long as $f(x)$ increases with x in a nonlinear manner (*e.g.*, we have checked $f(x) = ax + bx^2$).

Corresponding to the 'conservation law' of momentum flux, the relation $\frac{d\langle x_j\rangle_i}{dt} = \langle x_{j-1}\rangle_i - \langle x_j\rangle_i + \langle \beta_{j-1}\rangle_i$ holds, where $\langle\rangle_i$ denotes the average over the horizontal direction for the jth layer, $\langle x_j\rangle_i = \frac{1}{N}\sum_i x_{ij}$ and $\langle \beta_{j-1}\rangle_i = \frac{1}{N}\sum_i \beta_{ij-1} = 1$. Since the equation is governed by the relaxation term, the stress variables $x_{ij}(t)$ are attracted to a fixed point solution x^*_{ij}. As will be shown later, there is a huge number of stable fixed point solutions for the steady-state equation if $\alpha \gtrsim 0.7$. For a fixed point solution, the conservation law implies that $\langle x^*_j\rangle_i = \langle x^*_{j-1}\rangle_i + \langle \beta_{j-1}\rangle_i = \cdots = j+1$.

Now we study the history dependence on how the initial condition is prepared, by choosing the following operations for preparing the initial condition. We represent the process of piling as the addition of a weight $\beta_{ij} = 1$ at a site, while the stress variable x_{ij} then evolves from 0. Before piling a bead at a site, $\beta_{ij} = 0$ and $x_{ij} = 0$ are assigned. Then, in

*E-mail: shuji@complex.c.u-tokyo.ac.jp

order to simulate a piling process from the bottom to the top, at each step, we randomly choose a horizontal site i from a Gaussian distribution with the standard deviation $W \times (N/2)$ and take the largest value j such that the site (i,j) is not vacant. If both the neighboring lower sites are occupied, the weight β is added to that site. If at least one of the sites of the neighboring lower sites is vacant, this (mesoscopic) bead is added to the lower vacant site. By adding weights successively, the dynamics is iterated, leading to a fixed stress field.

Indeed, this operation is inspired by the sandpile experiments, where the pressure distribution at the bottom has a minimum in the center when the sand grains are piled from a small hole, while it has a maximum at the center when the sand grains are scattered during piling.[2,3] The case of $W \ll 1$ corresponds to a piling process from a thin hole, while the case of $W > 1$ corresponds to a piling process in which the beads are scattered.

Figure 1 shows the results of the stress field for (a) $W = 0.1$ and (b) $W = 10$. Note that stress x_{ij} is accumulated in a few lattice sites forming a downflow stream, and these sites form a connected chain, which we call 'stress chain', borrowing the term for granular matter. The accumulation of the stress itself is possible, since our model has a tendency to accumulate more stress at a site with a larger stress value. In fact, the formation of stress chains is commonly observed for $\alpha \gtrsim 0.7$.

As shown in Fig. 1, the stress chain is distributed around the edge for case (a), while in case (b), it is distributed around the center. The stress distribution at the bottom plate, obtained from an average of 100 samples, is plotted in Fig. 1(c). It has a dip at the center in case (a), while it is unimodal in case (b). The stress distribution with the dip is observed

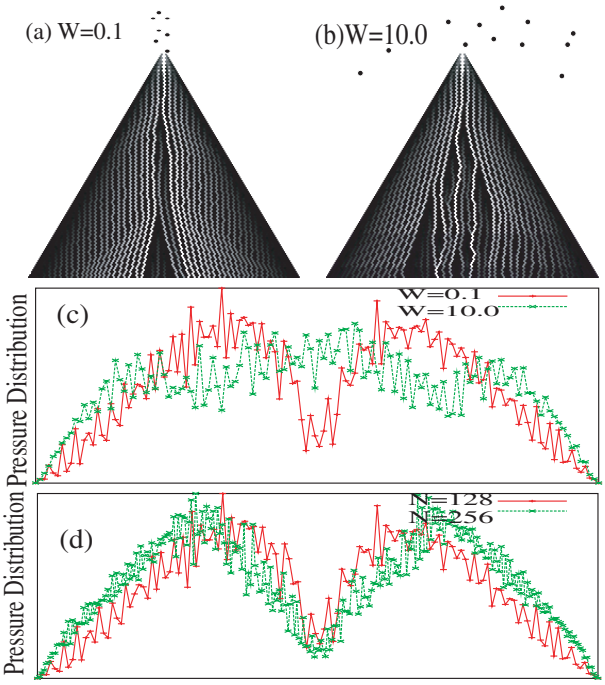

Fig. 1. Simulations of stress dynamics for (a) $W = 0.1$ and (b) $W = 10.0$. White pixels indicate large x^*_{ij} (i.e. $x^*_{ij} > \langle x^* \rangle_i$). (c) Distribution of x^*_{iM-1} obtained by averaging 100 samples for $W = 0.1$ (red line) and $W = 10.0$ (green line). (d) Scaled distribution for $N = 128$ and $N = 256$.

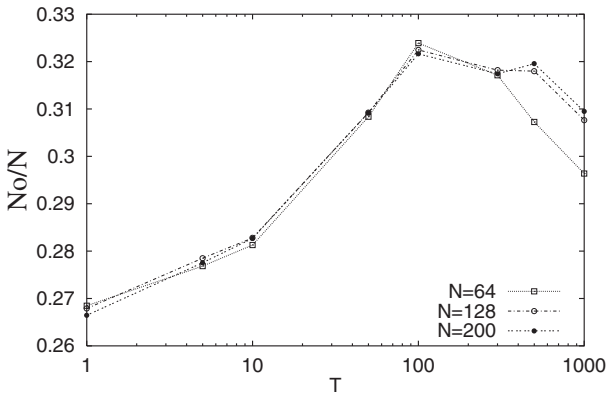

Fig. 2. The ratio of the number of stress chains to N plotted against the time scale T of the piling process described in the text. The vertical lattice size is 120, and the horizontal size is 64 (□), 128 (○), 200 (●). The results were obtained by averaging 500 runs.

independent of the system size and fits a scale-invariant form upon normalizing the width by its size, as shown by red points in Fig. 1(d).

As a second demonstration of history dependence, we study how the stress pattern depends on the time scale for the piling process. Differences in time scales are introduced as follows: first the system is again prepared in a "no-bead state", i.e., a state with $\beta_{ij} = x_{ij} = 0$ for all sites. Then, in each T step (until the top layer $j = 0$ is reached), we set $\beta = 1$ for all the sites in the lowest vacant layer simultaneously. The stress field x_{ij} of a new site is set to a random value in the range $[0, 0.1]$ to represent small fluctuations. Thus, with the help of eq. (1), a fixed stress pattern x^*_{ij} is obtained. The results are shown in Fig. 2.

Through this process, stress chains are again formed. We have computed the number of stress chains $\langle\langle N_o \rangle\rangle$ by counting the sites that satisfy $x^*_{ij} > \langle x^*_j \rangle_i = j + 1$ in the bottom layer, where $\langle\langle .. \rangle\rangle$ is the ensemble average over 500 trials. When the piling process is fast ($T < 10$), the number of stress chains is small, and in fact the stress is accumulated at few sites in the lower layer. For larger T, the number of stress chains is larger, and the weight is supported by more sites.[12] This dependence on the time scale is commonly observed for $\alpha > 1$. The time scale $T \approx 10$ is related to the intrinsic time scale for the relaxation of the coupled system, as will be discussed later.

Now we discuss the origin of this history dependence in terms of the dynamical systems theory. First, the coexistence of multiple attractors is confirmed by choosing different initial conditions with $x_{ij} \in [0, 1]$. Then after the relaxation is completed, we compute the patterns of the fixed point attractors. Depending on the value of α, we have the following three phases.

(I) $\alpha \lesssim 0.7$: The system is always attracted to a stable homogeneous state. A single stable fixed point with $x^*_{ij} = j + 1$ (independent of i) exists.

(II) $0.7 \lesssim \alpha \leq 1$: In addition to the homogeneous solution, many stable fixed point patterns appear [Fig. 3(a)]. In the upper region, the patterns are almost homogeneous while in the lower region they are striped (zigzag-like) with some dislocations. The homogeneous state is destabilized at lower layer because the state is convectively unstable as will be

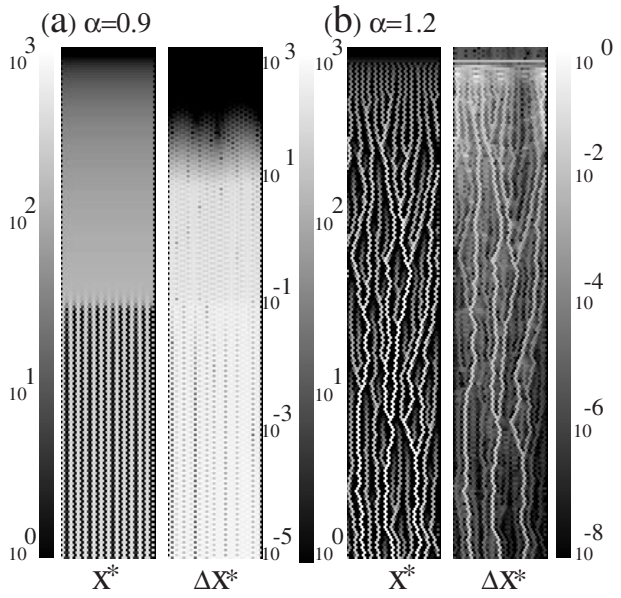

Fig. 3. The left columns in (a) and (b) show the stress variables x_{ij}^* plotted in gray scale for a system size of 32×200. (a) $\alpha = 0.9$ and (b) $\alpha = 1.2$. The right columns depict $\Delta x_{ij}^* = |x_{ij}^{*\prime} - x_{ij}^*|$ in gray scale, where $x_{ij}^{*\prime}$ is the fixed point reached after a perturbation is added as $\beta_0 = (1, 1, \dots) \to \beta_0 + \delta\beta$, with $\delta\beta \in [-0.00001, 0.00001]$.

shown later.

(III) $\alpha > 1$: The homogeneous solution becomes unstable at $\alpha = 1 + 1/(j+1)$, and further down stream it is always unstable. When following the layers down, the behavior changes from an almost homogeneous state to a stripe pattern, as in phase II, and then to patterns where stresses are accumulated into fewer sites forming inhomogeneous patterns, as shown in Fig. 3(b).

Although both phases II and III have multiple fixed points, the history dependence discussed so far is observed only for phase III. One important difference between phases II and III lies in the response of each attractor to a perturbation applied at the top layer.

In phase II, there is a switch from one attractor to another when applying a tiny perturbation for at least $O(1)$ time units. A local perturbation in an upper layer spreads out horizontally in the lower layers. Fig. 3(a) shows x_{ij}^* and the variation Δx_{ij}^* caused by the perturbation. As can be seen, x_{ij} are altered for almost all sites.

In phase III, a perturbation must be applied for a long time in order to cause a switch to a different attractor. Furthermore, the length with which the perturbation must be applied increases as the perturbation amplitude decreases. Here, a perturbation is not transferred smoothly to all sites, but is localized around a few stress chains. As shown in Fig. 3, the sites whose x_{ij} values are altered are located around the stress chains, particularly at the lower layers. The change of x_{ij}^* is temporally intermittent. After a perturbation is applied, the stress values remain almost constant, but then for some sites, they show a sudden increase corresponding to a rearrangement of the stress chains.

In order to study the relationship between the response to a perturbation and history dependence, we carried out the following simulations. After the system reaches a fixed point, we apply a perturbation at the top (0-th) layer to change $\boldsymbol{\beta}_0 = (1, 1, \dots)$ to $\boldsymbol{\beta}_0 + \delta\boldsymbol{\beta}_0$ over τ steps, where $\delta\boldsymbol{\beta}_0$ is chosen randomly over $[-\epsilon, \epsilon]$ and fixed. After waiting for the system to settle down to a fixed point attractor, we checked whether or not it is identical to the original attractor. By taking 100 samples, the ratio of attractor switching is computed as a function of perturbation strength ϵ and perturbation duration τ. This is shown in Fig. 4 for phase III. As the duration τ of the application of the perturbation increases, its effect accumulates, causing a switch from one attractor to another. The required time for a given switch ratio is approximately $1/\epsilon$. Hence the history dependence in Fig. 2 is a natural consequence of the above time-scale dependence. Note that for phase II, no dependence on τ or ϵ is observed since almost all perturbations kick the system to a different attractor.

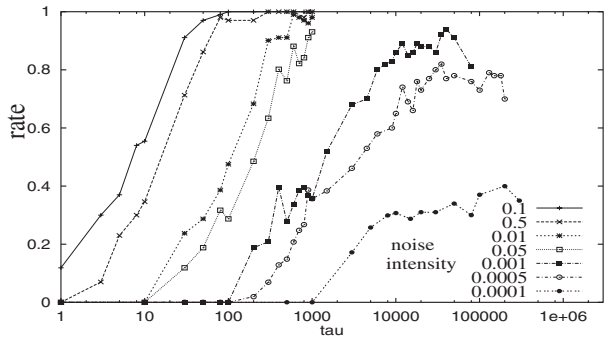

Fig. 4. The fraction of attractor switches due to a perturbation with amplitude $\epsilon \in [0.0001, 0.1]$, and duration τ in the top layer. The lattice size is 32×200 and $\alpha = 1.2$.

The response of a system to tiny perturbations is generally studied by means of a Lyapunov analysis. Ordinary Lyapunov analysis, however, is not useful here, since all the fixed points studied so far are linearly stable. Rather, in an open-flow system, the co-moving Lyapunov exponent for measuring how a perturbation is amplified along the spatial direction is important.[13–16]

In order to discuss the stability along the spatial direction, we first obtain the relationship between the fixed point at the $(j-1)$-th layer and that at the j-th layer $\boldsymbol{x}_j^* = \boldsymbol{f}(\boldsymbol{x}_{j-1}^*, \boldsymbol{x}_j^*)$ by setting the r.h.s. of eq. (1) to 0. This gives a spatial map from $\boldsymbol{x}_{j-1}^*$ to $\boldsymbol{x}_j^*$. The amplification rate of the perturbation δx_{j-1}^* at the $(j-1)$-th layer is given by $\delta x_j^* = M_j \delta x_{j-1}^*$, with M_j as the Jacobi matrix for the spatial map.

The rate at which a perturbation expands in the downflow direction is then given by the maximal Lyapunov exponent of the spatial map as $\lambda_j^{\mathrm{sp}} = \log(\mu_j)/j$, where μ_j is the square root of the maximal eigenvalue of $Q_j^\dagger Q_j$, with $Q_j = M_j M_{j-1} \dots M_1$, where j starts from the 0-th layer. The local expansion rate from one layer to the next ($\lambda_j^{\mathrm{loc.}}$) is also computed as the logarithm of the square root of the maximal eigenvalue of $M_j^\dagger M_j$. We plotted λ_j^{sp} in Fig. 5 as a function of j.

In phases II and III ($\alpha = 0.8, 1.2$) $\lambda_j^{\mathrm{loc.}}$ is positive, and a perturbation in one layer is amplified to the next. The behavior of λ_j^{sp}, however, is different between the two phases. In phase II, λ_j^{sp} increases with layer j, in fact, the attractors of phase II are convectively unstable.[13–15] On the other hand, in phase III, λ_j^{sp} first increases sharply and then

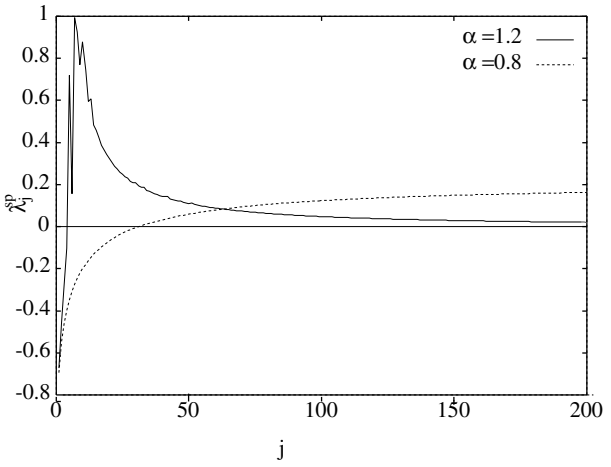

Fig. 5. Spatial Lyapunov exponent λ_j^{sp} for $\alpha = 0.8$ (- - -) and 1.2 (—). See text for definition. The lattice size is 32×200.

decreases towards 0 as j is increased. Hence, a perturbation in the top layer may not reach the bottom layer if the number of layers is sufficiently large.

This property is important for explaining the history dependence shown in the piling process. Since the local exponent is positive, a perturbation in the piling process is amplified to the next layer, and leads to a variety of stress patterns. With the piling process, the distance between the top and the bottom layers increases, and a perturbation caused by the addition of a layer at the top has less influence on the bottom because λ_j^{sp} approaches zero. The lower layers are thus 'protected' from the changes at the top layers. Hence a given stress pattern selected in the initial stage is 'memorized'. This leads to the history dependence in phase III, while for phase II, a perturbation in the top layer is continuously amplified to the bottom layer, resulting no history dependence.

In conclusion, we constructed a simple model that exhibits history dependence, where 'memory' is embedded successively to downflow states. The condition for history dependence is discussed from the viewpoint of a response to perturbations. When there is a strong constraint on the attractors that can be reached by a perturbation to a given attractor, history dependence is observed, while if the perturbation influences all sites globally, history dependence is not possible.[17] This condition for history dependence was further characterized by analyzing the spatial Lyapunov exponent.

The history dependence thus observed is a general property of dynamical systems, as long as there is self-reinforcement of stress. It will be interesting to pursue the possibility that the present mechanism may underlie the sandpile history dependence, since the results of the pressure ditribution if Fig. 1 agree qualitatively with the observations obtained in previous sandpile experiments.[2,3] Of course, it is important to generalize the results of the present study for applicability to other history dependent phenomena including biological systems.

The authors would like to thank S. Sasa, K. Fujimoto, and A. Awazu for discussions. We also thank F. H. Willeboordse for critical reading of the manuscript. This research was supported by Grants-in-Aid for Scientific Research (11CE2006).

1) H. M. Jaeger, S. R. Nagel and R. B. Behringer: Rev. Mod. Phys. **68** (1996) 1259.
2) L. Vanel, D. Howell, D. Clark, R. P. Behringer and E. Clément: Phys. Rev. E **60** (1999) R5040.
3) J. Geng, E. Longhi, R. P. Behringer and D. W. Howell: Phys. Rev. E **64** (2001) R060301.
4) S. J. Savage: *Powders & Grains '97*, ed. R. P. Behringer and J. T. Jenkins (Balkema, Rotterdam, 1997) p. 185.
5) J. Smid and J. Novosad: Int. Chem. Eng. Symp. Ser. **1** (1971) 291.
6) J.-P. Bouchaud, M. E. Cates and P. Claudin: J. Phys. I (Paris) **5** (1995) 639.
7) M. E. Cates, J. P. Wittmer, J.-P. Bouchaud and P. Claudin: Philos. Trans. R. Soc. London **356** (1998) 2535.
8) S. F. Edwards and C. C. Mounfield: Physica A **226** (1996) 25.
9) H. G. Mattutitis *et al.*: Proc. RIMS Symp. Mathematical Apsects of Complex Fluids II, RIMS Kokyoroku series 1188 (2000) p. 123.
10) This type of model is introduced in S. N. CopperSmith *et al.*: Phys. Rev. E **53** (1996) 4673, which is a stochastic model at the microscopic level. Ours is the deterministic model at a mesoscopic scale. Although the q-model successfully reproduces the the exponential force distribution observed in the sandpile experiments, history dependence is not explained.
11) It is not known if such self-reinforcement exists in the sandpile experiment, but it may be interesting to search for it.
12) For larger T, it seems that the number of stress chains slightly decreases; the reason for this is not yet known.
13) R. Deissler and K. Kaneko: Phys. Lett. A **119** (1987) 397.
14) K. Kaneko: Physica D **23** (1886) 436.
15) F. H. Willeboordse and K. Kaneko: Physica D **86** (1995) 428.
16) D. Vergni, M. Falcioni and A. Vulpiani: Phys. Rev. E **56** (1997) 6170.
17) For this type of correlated switching among attractors, see, K. Kaneko: *Theory and Applications of Cellular Automata*, ed. S. Wolfram (Worlds Scientific., Singapore, 1986).